Targeting stromal interactions in the pro-metastatic tumor microenvironment : Endoglin & TGF-beta as (un)usual suspects

Paauwe, M.

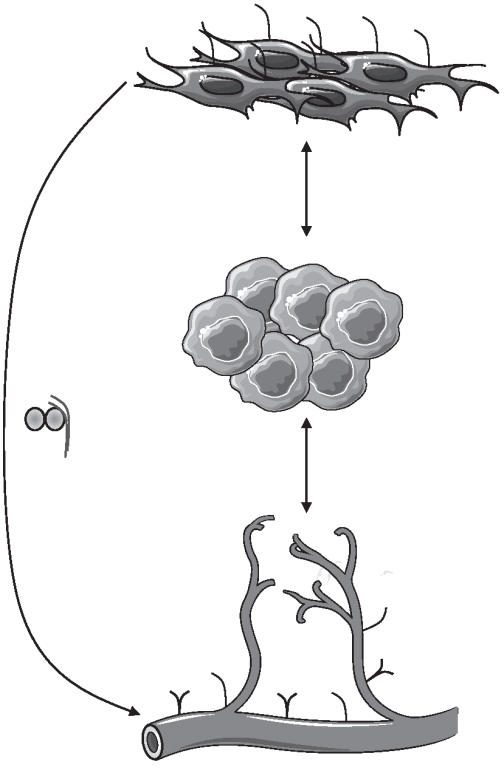

Chapter 5

Endoglin targeting inhibits tumor angiogenesis and metastatic spread in breast cancer

Madelon Paauwe[1,2], Renier C. Heijkants[1], Charlotte H. Oudt[1], Gabi W. van Pelt[3], Chao Cui[1], Charles P. Theuer[4], James Hardwick[2], Cornelis F.M. Sier[2,3], Lukas J.A.C. Hawinkels[1,2]

Leiden University Medical Center, Depts. of [1]Molecular Cell Biology, [2]Gastroenterology-Hepatology and [3]Surgery, Leiden, the Netherlands; [4]Tracon Pharmaceuticals, San Diego, CA, USA

Oncogene, 2016;35:4069-4079

Abstract

Endoglin, a transforming growth factor-β co-receptor, is highly expressed on angiogenic endothelial cells in solid tumors. Therefore, targeting endoglin is currently being explored in clinical trials for anti-angiogenic therapy. In this project, the redundancy between endoglin and vascular endothelial growth factor (VEGF) signaling in angiogenesis and the effects of targeting both pathways on breast cancer metastasis were explored.

In patient samples, increased endoglin signaling after VEGF inhibition was observed. *In vitro* TRC105, an endoglin neutralizing antibody, increased VEGF signaling in endothelial cells. Moreover, combined targeting of the endoglin and VEGF pathway, with the VEGF receptor kinase inhibitor SU5416, increased anti-angiogenic effects *in vitro* and in a zebrafish angiogenesis model. Next, in a mouse model for invasive lobular breast cancer, the effects of TRC105 and SU5416 on tumor growth and metastasis were explored. Although TRC105 and SU5416 decreased tumor vascular density, tumor volume was unaffected. Strikingly, in mice treated with TRC105, or TRC105 and SU5416 combined, a strong inhibition in the number of metastases was seen. Moreover, upon resection of the primary tumor, strong inhibition of metastatic spread by TRC105 was observed in an adjuvant setting. To confirm these data, we assessed the effects of endoglin-Fc (an endoglin ligand trap) on metastasis formation. Similar to treatment with TRC105 in the resection model, endoglin-Fc expressing tumors showed strong inhibition of distant metastases.

These results show, for the first time, that targeting endoglin, either with neutralizing antibodies or a ligand trap, strongly inhibits metastatic spread of breast cancer *in vivo*.

Introduction

Breast cancer is the second most common form of cancer globally, with over 1.5 million diagnosed patients in 2012 (1). Primary treatment for breast cancer patients is surgical removal of the tumor, complemented with adjuvant therapies like (chemo-)radiation or anti-angiogenic therapies. The formation of a vascular network, called angiogenesis, is crucial for solid tumors to sustain oxygen and nutrient supply, but also indispensable for their metastatic spread (2, 3). Therefore, anti-angiogenic therapies have been developed for the treatment of solid cancers. Vascular endothelial growth factor (VEGF) is one of the major players in the induction of angiogenesis and therefore many anti-angiogenic agents have been developed against VEGF (4). Although preclinical data of the first VEGF neutralizing antibody bevacizumab were promising, the efficacy in the clinic was limited, leading to withdrawal of the FDA approval as adjuvant therapy for breast cancer (5). In addition to antibodies, kinase inhibitors like SU5416 (Semaxanib), a selective VEGF receptor tyrosine kinase inhibitor, have been developed. SU5416 was used as an adjuvant treatment in patients with advanced colorectal cancer, but the phase-III trial was halted due to a lack of clinical benefit (NCT00021281). A phase-I clinical trial for SU5416 in inflammatory breast cancer has been completed in 2010, but no results have been reported thus far (NCT00005822). The limited clinical benefit of anti-angiogenic therapies is most likely caused by therapy resistance (6), characterized by an initial response to treatment followed by patient relapse. This can be caused by upregulation of alternative pro-angiogenic signaling pathways (7), for example the endoglin/transforming growth factor (TGF)-β pathway.

Endoglin is a co-receptor for TGF-β and bone morphogenetic protein (BMP)-9 and is highly expressed on angiogenic endothelial cells (8-10). Endoglin is indispensable for developmental angiogenesis as has been shown by embryonic lethality of endoglin knockout mice (11-13). In cancer, previous studies have shown a clear correlation between endoglin microvessel density and patient survival (14-17). BMP-9 and TGF-β can, upon binding to endoglin, induce phosphorylation of downstream Smad proteins, inducing an angiogenic phenotype (18). TRC105 is a chimeric IgG1 monoclonal antibody that binds human endoglin with high affinity and is currently being tested in clinical trials as anti-angiogenic therapy (19). TRC105 prevents BMP-9 binding to endoglin and induces an antibody-dependent cytotoxicity response leading to apoptosis of endoglin expressing cells (20). Results of a phase-I clinical trial showed safety of the antibody in patients with various solid cancers, and in two patients even clinical benefit was observed for a prolonged period of time (19). Recently, a phase-IB clinical trial was completed showing that the combination of TRC105 and bevacizumab was safe and even resulted in reduced tumor volumes in some bevacizumab resistant patients (21).

In the present study, we have assessed the inhibition of angiogenesis by simultaneous targeting of the endoglin and VEGF pathway. *In vitro* and *in vivo* angiogenesis models and an orthotopic breast cancer mouse model show increased inhibition of angiogenesis by

combining TRC105 and SU5416. Even more striking, endoglin targeting, using a neutralizing antibody or ligand trap, strongly inhibits the metastatic spread of breast cancer cells.

Materials and methods

Patient samples

Paraffin-embedded tissue samples were obtained from the Department of Surgery, Leiden University Medical Center. The patient population contained stage I-IV rectal cancer patients treated in a neo-adjuvant setting with bevacizumab. Samples were pre-surgery tumor biopsies (N=5) and tumor tissue obtained after surgery (N=3). Additionally, tumor tissue samples from patients treated with only chemoradiation therapy (N=8) or a combination of chemoradiation and bevacizumab (N=11) were evaluated. Patient characteristics and follow-up were recorded by the Department of Surgery. Samples were used according to the guidelines of the Medical Ethics Committee of the Leiden University Medical Center.

Tissue analysis

Immunohistochemical stainings were performed as described before (22) using antibodies against CD31 (Santa Cruz Biotechnologies, USA), endoglin (R&D Systems, Abington, UK) or phosphorylated Smad1 (Cell Signaling Technologies, USA). Four representative fields per tumor slide were photographed with a Leitz Diaplan microscope (Leitz, Wetzlar, Germany) and staining was quantified using ImageJ software. ELISA analysis for mouse VEGF was performed according to the manufacturers instruction (DY493, R&D systems). BMP-9 ELISA and QPCR analysis were performed as described before (23, 24). Primers are described in supplementary table S1.

Cell culture and signaling assays

Primary human umbilical vein endothelial cells (HUVECs) were cultured as described before (25). P53/E-cadherin double knockout mouse breast cancer cells (KEP 1-11, (26)) were cultured as described before (27).

$3x10^5$ HUVEC cells were seeded in gelatin coated 6 well plates. Upon 90% confluency, cells were serum starved overnight in medium containing either 40 µg/mL TRC105 (Tracon Pharmaceuticals, San Diego, CA, USA) or 40 µg/mL human IgG (BioXCell, West Lebanon, NH, USA). 30 minutes before stimulation, 0.1% dimethyl sulfoxide (DMSO, as solvent control) or 1 µM SU5416 (WuXi app tec, Shanghai, China) was added, followed by a 10 minute stimulation with either 0.1 ng/mL recombinant human (rh)BMP-9 (R&D Systems, Abington, UK), 5 ng/mL TGF-β3 (28) or 50 ng/mL rhVEGF (Peprotech, London, UK). For TGF-β signaling studies, HUVECs were starved overnight in the presence of TRC105, IgG, the ALK-5 inhibitor SB431542 (Tocris, Bristol, UK) or combinations. Next day, cells were stimulated with 5 ng/mL TGF-β3. Cells were lysed in RIPA buffer (150 mM NaCl, 1% NP-40, 0.25% deoxycholate, 0.1% SDS, 50 mM Tris (pH 8.0), 2 mM EDTA, 1 mM NaVO4, 10 mM NaF

and 1 mM sodium orthovandate (BDH Laboratory, Poole Dorstet, UK)), protein content was determined and western blot analysis was performed as described before (24). Membranes were incubated overnight with primary antibodies against endoglin (R&D Systems), phosphorylated Smad1, phosphorylated Smad2, phosphorylated VEGFR2 Tyr1175 (all Cell Signaling technologies) or phosphorylated ERK1/2 (Sigma Aldrich). Blots were stripped and re-probed with either mouse anti-GAPDH (Millipore, Amsterdam, The Netherlands) or mouse anti-β-actin (Sigma Aldrich) antibodies as loading controls. Densitometry analysis was performed using ImageJ software.

MTS proliferation assay

HUVECs (2500 cells/well) were seeded in 96-well plates in triplicates. After 16 hours, medium was replaced with 100 µL medium supplemented with 40 µg/mL TRC105, 1 µM SU5416 or controls. Additionally, the assay was also performed in serum-free (SF) medium, containing bovine pituitary extract, and in the presence of 50 ng/mL rhVEGF or 0.1 ng/mL BMP-9. At indicated time points 20 µL MTS substrate (Promega, Madison, USA) was added to each well and absorbance was measured at 490 nm (Perkin Elmer, Groningen, The Netherlands).

In vitro angiogenesis assays

HUVECs were resuspended in M199 medium, supplemented with 5% FCS and 0.2% heparin. $2x10^4$ HUVECs were seeded in matrigel (BD Biosciences) coated 96-well plates in presence of 40 µg/mL TRC105, 1 µM SU5416 or controls. After 16 hour incubation, five images per well were acquired at 40x magnification. The number of branches per branchpoint and the number of closed polygons were analyzed, in a blinded manner by two independent observers.

The endothelial sprouting assay was performed as described before (29). In short, HUVEC spheroids were embedded in collagen-I containing 0% or 20% FCS, and supplemented with 40 µg/mL TRC105, 1 µM SU5416 or controls. Images were acquired after overnight incubation and average sprout length was calculated using ImageJ software.

Zebrafish

TRC105 and human IgG were labeled with Dyelight 594 NHS-Ester fluorescent dye (Life Technologies Europe, Bleiswijk, The Netherlands) and 1 ng antibody was injected in the blood island of two day old Fli:eGFP zebrafish embryos. Two days after injection, embryos were fixed and green and red fluorescent signals were analyzed. For angiogenesis assays Fli:eGFP transgenic zebrafish were injected in the blood island 28 hours post fertilization with either 1 ng human IgG or TRC105. SU5416 (0.5 mg/mL) or DMSO was supplied in the fish water. Zebrafish embryos were analyzed 3 days post fertilization using confocal microscopy (Leica TCS-SP5 STED).

Mouse breast cancer model

All animal experiments were approved by the Dutch animal ethics committee. Nine week old female Balb/c nu/nu mice (Charles River, L'Arbresle Cedex, France) were anaesthetized and $3x10^5$ luciferase expressing KEP1-11 cells were injected in the 4th mammary gland as described before (27). Mice were injected IP with 100 mg/kg luciferin, and imaged on the IVIS Lumina-II (Caliper Life sciences, Hopkinton, USA). Animals were treated twice weekly starting at week 2 after transplantation with 0.9% NaCl, 15 mg/kg human IgG and DMSO, 50 mg/kg SU5416 and 15 mg/kg human IgG, 15 mg/kg TRC105 and DMSO or 15 mg/kg TRC105 and 50 mg/kg SU5416, IP. Time between treatment with DMSO or SU5416 and human IgG or TRC105 was at least 24 hours. Tumor volume was measured twice weekly using a caliper and calculated (tumor volume = $(width^2 * length)/2$). After six weeks, mice were sacrificed and blood and tissue samples were collected.

For the tumor resection model, tumors were transplanted as described above and allowed to grow for four weeks. Mice were anaesthetized with KSA and the primary tumor was resected (30). Complete removal of the tumor was confirmed by bioluminescent imaging. Twice weekly adjuvant treatments with either 15 mg/kg human IgG or TRC105 were started one week after tumor resection (Fig. 6A). Mice were imaged weekly for an additional 6 weeks to determine metastatic spread.

Orthotopic breast cancer using stable cell lines

Fc and Endoglin-Fc (a fusion protein consisting of the endoglin extracellular domain and Fc region of an antibody) expressing plasmids were cloned into lentiviral expression vectors. Stable cell lines were generated by puromycin selection (5 µg/mL, Sigma-Aldrich). Expression of the constructs was confirmed using western blot. Transplantation, resection and imaging of the tumors were performed as described above. Mice were sacrificed after 7 weeks (primary tumor) or 10 weeks (resection).

Statistical analysis

Differences between two groups were calculated using Student's t-test. Survival curves were generated using Kaplan-Meier analysis and the Log Rank test. P-values below 0.05 were considered significant.

Results

Anti-VEGF treatment in patients increases endothelial Smad1 phosphorylation

First, the potential redundancy between the endoglin and VEGF pathway in angiogenesis was examined. We had access to a small cohort of rectal cancer patients treated in a neo-adjuvant setting with anti-VEGF therapy (bevacizumab), providing us with pre-treatment biopsies and post-treatment resection specimens. Tissue sections from

patients treated with bevacizumab were stained for phosphorylated Smad1 (pSmad1), the major signaling molecule downstream of endoglin. Pre-treatment biopsies (Fig. 1A, upper panel) showed limited staining for pSmad1 in the endothelial nuclei compared with the resection specimen from the same patient after bevacizumab, where almost all endothelial nuclei showed strong pSmad1 accumulation (Fig. 1A, lower panel). To exclude that this observation was due to the difference of biopsies versus resection specimens, a group of patients that only received chemoradiation therapy (standard of care, Fig. 1B, upper panel) was compared with a group receiving both chemoradiation therapy and bevacizumab (Fig. 1B, lower panel). These data confirmed increased nuclear accumulation of pSmad1 in endothelial cells upon anti-VEGF therapy. These results indicate that upon VEGF inhibition alternative pathways, like the endoglin pathway, seem to be upregulated in cancer patients.

Endoglin and VEGF pathways are connected *in vitro*

Next, we examined whether redundancy could also be observed between endoglin and VEGF pathways *in vitro*. Human umbilical vein endothelial cells (HUVEC) were stimulated with VEGF or BMP-9, the main endoglin ligand. Treatment with BMP-9 induced rapid Smad1 phosphorylation, which could transiently be inhibited by TRC105 (Fig. 2A). In addition to inhibiting Smad1 phosphorylation, TRC105 increased phosphorylation of the anti-angiogenic Smad2 (Fig. 2B, left panel and supplementary Fig. S1A) similar to stimulation with 5 ng/mL TGF-β (Fig. 2B, right panel). Smad2 phosphorylation was dependent on ALK-5 kinase activity, since treatment with the kinase inhibitor SB431542 abrogated TRC105-induced Smad2 phosphorylation (Fig. 2B, right panel). These data indicate a shift towards an anti-angiogenic response by TRC105. VEGF induced rapid ERK phosphorylation in HUVECs, which could be inhibited by SU5416 (Fig. 2C). Interestingly, when HUVECs were treated with TRC105 and subsequently stimulated with VEGF, we observed increased ERK phosphorylation, compared to VEGF stimulation without TRC105 pre-treatment (Fig. 2D and supplementary Fig. S1B). This did not seem to be due to increased VEGFR2 Tyr1175 phosphorylation (supplementary Fig. S1C). These results suggest a connection between the endoglin and VEGF signaling pathways in endothelial cells.

Combined endoglin and VEGF targeting inhibits angiogenesis

If there is redundancy between the endoglin and VEGF pathways, simultaneous inhibition of both pathways could result in increased and sustained anti-angiogenic responses. Therefore, we assessed the effects of TRC105, SU5416, and combination treatment on *in vitro* proliferation, migration and angiogenesis. TRC105 did not significantly affect HUVEC proliferation, whereas both SU5416 and the combination treatment resulted in statistically significant inhibition of HUVEC proliferation (Fig. 3A). Under serum-free (SF) conditions (Fig. 3B), or SF-medium supplemented with either VEGF of BMP-9 (supplementary Fig. S2) we observed the same inhibitory effects on proliferation of HUVECs by SU5416 and combination treatment, albeit more pronounced. In contrast to BMP-9, VEGF enhanced

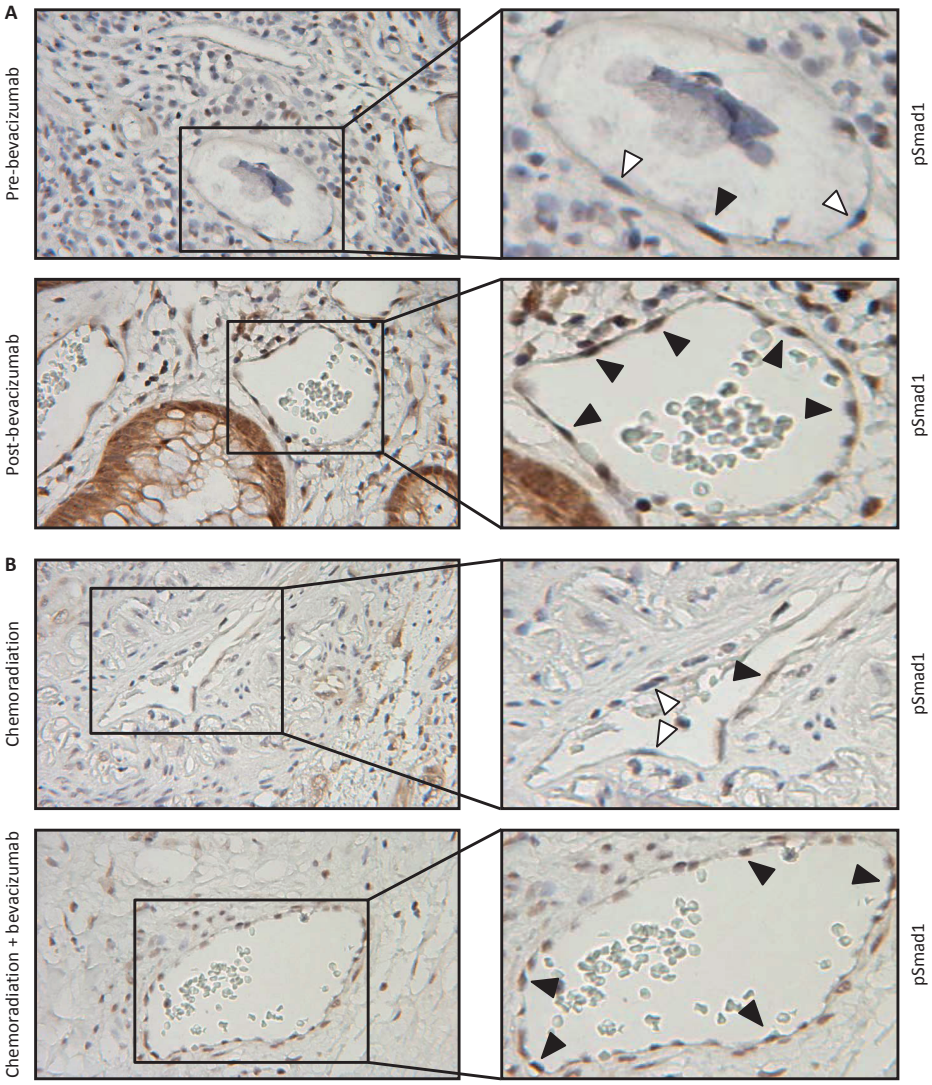

Figure 1 Anti-VEGF treatment results in increased Smad1 phosphorylation. A. Immunohistochemical staining for phosphorylated Smad1 (pSmad1) revealed increased endothelial nuclear pSmad1 in tissue samples from patients treated with bevacizumab (lower panel) compared with pre-treatment tumor biopsies (upper panel). B. Treatment with bevacizumab in combination with chemoradiation therapy (lower panel) increased pSmad1 in endothelial nuclei compared with chemoradiation treatment only (upper panel). White arrowheads; pSmad1 negative nuclei. Black arrowheads; pSmad1 positive nuclei. Magnification x200, right panels x400.

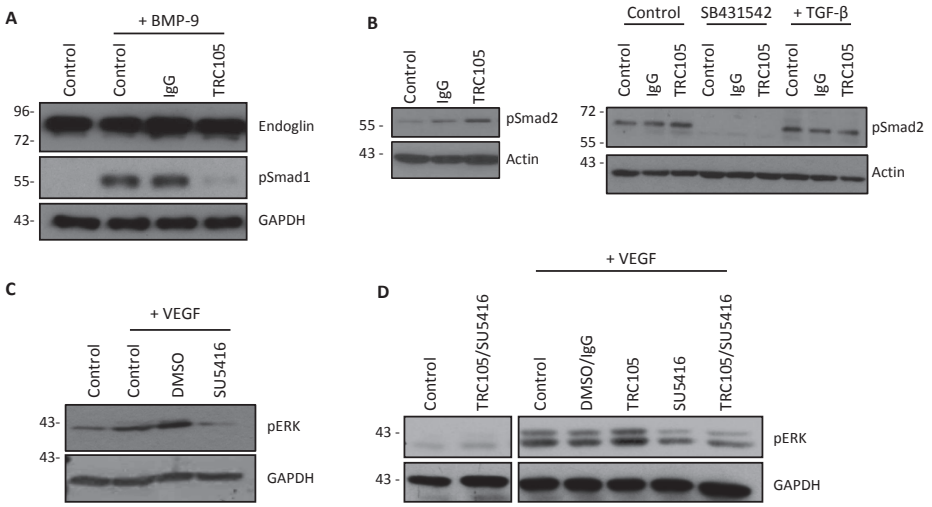

Figure 2 Redundancy between endoglin and VEGF signaling in HUVECs *in vitro.* A. BMP-9 stimulation (10 min) induced strong Smad1 phosphorylation (pSmad1) in HUVEC cells, which is inhibited by TRC105. B. Overnight treatment with TRC105 increased Smad2 phosphorylation (pSmad2, left panel), to a comparable level as induced by TGF-β (1h). This effect was completely blocked by the ALK-5 kinase inhibitor SB431542 (right panel). C. VEGF stimulation (10 min) increased ERK1/2 phosphorylation (pERK), which can be inhibited by SU5416. D. Pre-treatment with TRC105 increased VEGF-induced pERK, which can be reverted by SU5416 or TRC105/SU5416 combination therapy. All western blots are representative of three independent experiments.

HUVEC proliferation (Fig. 3C), underlining the importance of VEGF for endothelial cell proliferation *in vitro.*

Since, next to proliferation, migration of endothelial cells plays and additional role in angiogenesis, the cord forming ability of HUVECs in the presence of the inhibitors was assessed. First, we optimized the percentage of FCS in the medium for this assay, which was shown to be 5% (supplementary Fig. S3A). TRC105 did not significantly inhibit the number of closed polygons (Fig. 3D), nor the number of branches per branchpoint (supplementary Fig. S3B), while SU5416 strongly inhibited both read-outs of the angiogenic potential. Without further decreasing the number of closed polygons, additional effects of TRC105/SU5416 treatment on the cord morphology and integrity of the remaining cords were observed. The cell aggregates which were formed were less dense and appeared to disintegrate faster than in the other conditions. Next, angiogenic potential in a more complex 3-dimensional spheroid model for angiogenesis was assessed. HUVEC spheroids were embedded in the presence of the inhibitors, stimulated and average sprout length was determined (supplementary Fig. S3C). TRC105 did not affect endothelial sprouting (Fig. 3E), confirming the results of the cord formation assay. A trend towards decreased average sprout length was observed for SU5416, while combination treatment resulted in statistically significant decreased HUVEC sprouting (Fig. 3E). These data indicate that endothelial sprouting is more efficiently inhibited by a TRC105/SU5416 combination.

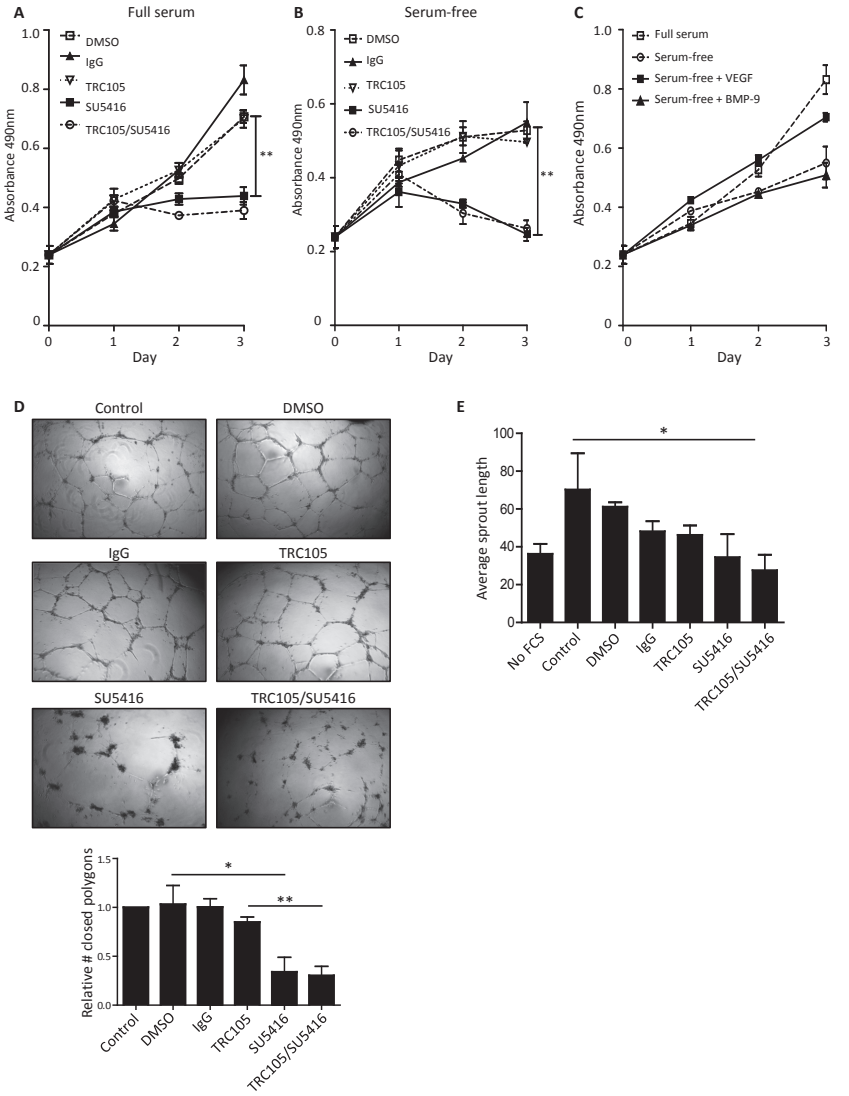

Figure 3 TRC105/SU5416 combination therapy enhances anti-angiogenic effects. TRC105 does not inhibit HUVEC proliferation in an MTS proliferation assay, while SU5416 and TRC105/SU5416 combination significantly decrease proliferation, in both full serum (A) and serum-free conditions (B). VEGF, either supplemented or BPE-derived, stimulates HUVEC proliferation, while BMP-9 did not show an effect (C). Data represent mean of two independent experiments performed in triplicate. D. HUVEC endothelial cells were seeded on matrigel and allowed to form endothelial cords. Endothelial cord forming capacity of HUVECs was assessed after overnight incubation with the inhibitors. TRC105 did not affect cord formation, whereas SU5416 treatment decreased the number of closed polygons. TRC105/SU5416 combination enhanced these effects on cord morphology, but not on the number of closed polygons. Data are normalized to control and represent mean of three independent experiments performed in triplicate. E. In 3-dimensional HUVEC sprouting assays sprouting of HUVECs was not affected by TRC105, while SU5416 and especially the TRC105/SU5416 combination significantly reduced sprouting. Data represent mean of three independent experiments, performed in triplicate. (*, P≤0.05, **, P≤0.01)

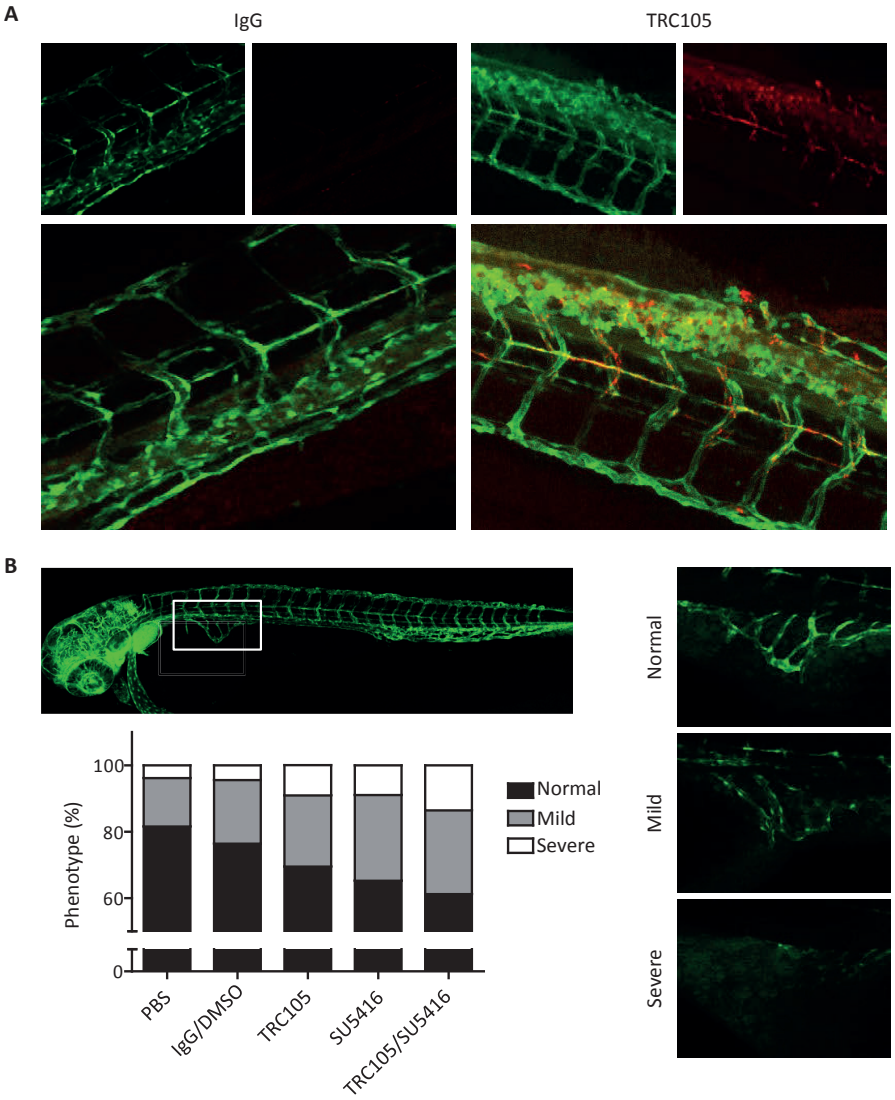

Figure 4 TRC105/SU5416 treatment inhibits angiogenesis in zebrafish. A. Two day old zebrafish embryos were injected with red fluorescently labeled human IgG or TRC105. TRC105 showed binding to GFP expressing zebrafish vasculature (right panel), whereas the IgG control did not show any fluorescent signal (left panel). B. Development of the subintestinal vessels (SIV) was assessed after two days of treatment with either TRC105, SU5416 or the combination. The SIV were scored as normal phenotype, or mildly or severely affected. TRC105 and SU5416 both increased the affected phenotypes, whereas TRC105/SU5416 combination enhanced this effect even more. Data represent mean percentage of fish with the observed phenotype from three independent experiments (n=38-114 fish/group/experiment).

TRC105/SU5416 combination enhances angiogenesis inhibition in zebrafish

To further study the effect of inhibiting VEGF and endoglin in a multicellular model for angiogenesis, we used Fli:eGFP zebrafish, in which all blood vessels express GFP. First, we analyzed whether TRC105, raised against human endoglin, was able to bind zebrafish endoglin. Human IgG (negative control) and TRC105 were fluorescently labeled and injected into zebrafish embryos. Two days after injection, TRC105 (red) co-localized with the GFP-expressing zebrafish endothelium, whereas no red fluorescent signal was observed in the IgG control (Fig 4A), implying that TRC105 binds to the zebrafish endothelium. Next, we determined the anti-angiogenic effects of combination treatment. Zebrafish embryos were injected with TRC105, while SU5416 was applied via the fish water. Two days after treatment, the phenotype of the subintestinal vessels was scored as either normal, mildly, or severely affected (Fig. 4B). Both TRC105 and SU5416 monotherapy increased the frequency of mainly the severe phenotype (from 4.4% to 9.1% (TRC105) and 9.0% (SU5416), Fig. 4B), while normal vessel development was decreased further after treatment with the TRC105/SU5416 combination (from 81.6% to 61.2%, Fig. 4B). These data show increased inhibition of angiogenesis in zebrafish embryos with combined endoglin and VEGF targeting.

Combined targeting of the endoglin and VEGF pathway inhibits tumor angiogenesis *in vivo*

Next, we evaluated the effects of TRC105/SU5416 combination treatment in a mouse model for invasive lobular breast cancer. Luciferase expressing KEP1-11 mouse breast cancer cells (26) were transplanted into the mouse mammary gland. Tumor growth and metastasis were followed by *in vivo* bioluminescent imaging (BLI). The data showed that neither treatment with TRC105 nor SU5416, nor combination treatment affected tumor volume assessed by luciferase signal (Fig. 5A) or caliper measurement (Fig. 5B). Treatment with TRC105 or TRC105/SU5416 combination increased VEGF expression in tumor homogenates (supplementary Fig. S4A), whereas VEGF plasma levels were only increased upon TRC105 treatment (supplementary Fig. S4B). Using quantitative PCR, enhanced endoglin expression was observed after SU5416 and combination treatment (supplementary Fig. S4C). Next, tumor vascularization was assessed by CD31 and endoglin staining. Vascular density was decreased by both TRC105 and SU5416, but the effects were significantly enhanced upon combination treatment (Fig. 5C/5D). Interestingly, the inhibitory effects of TRC105 on microvessel density determined by endoglin were stronger than determined by CD31, indicating specific targeting of endoglin expressing vessels. Staining for smooth muscle actin (SMA) positive cancer-associated fibroblasts (CAFs) revealed strongly reduced numbers of CAFs only in the TRC105 and combination treatment groups (Fig. 5E). Furthermore, a dramatic reduction in metastases was observed upon TRC105 monotherapy or in combination with SU5416 (Fig. 5F). SU5416 monotherapy did not reduce metastatic spread. Taken together, these data show enhanced inhibition of tumor angiogenesis by a combination of TRC105 and SU5416. Importantly, TRC105 seems to have a strong inhibitory effect on metastatic spread.

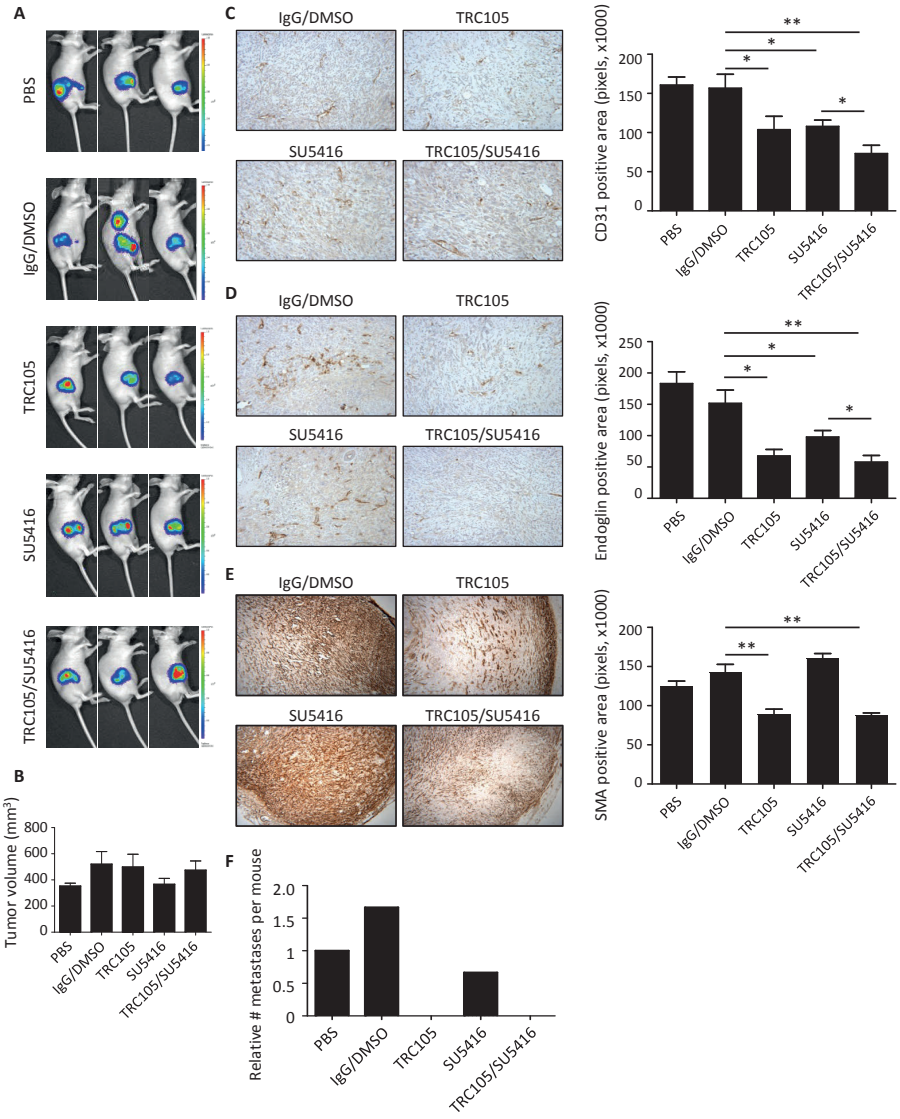

Figure 5 Combined targeting of endoglin and VEGF decreases tumor vascular density and metastatic spread of mouse breast cancer. KEP1-11 breast cancer cells were orthotopically transplanted and tumor growth was followed for six weeks using bioluminescent imaging (A) and caliper measurements (B). At the end of the experiment (6 weeks) tumor volume was not affected by the treatment, while tumor vascular density (CD31 (C) and endoglin (D) immunohistochemical staining) was strongly reduced upon TRC105 or SU5416 treatment, and even further decreased by TRC105/SU5416 combination. E. SMA+ stroma content of tumors was significantly reduced upon treatment with TRC105, either as monotherapy or in combination with SU5416 (n= 4-6 mice/group, average number of positive pixels). F. Mice treated with TRC105, either as monotherapy or in combination with SU5416, show a decreased number of metastases (six weeks after start of experiment, n= 4-6 mice/group). (*, P≤0.05, **, P≤0.01)

TRC105 inhibits breast cancer metastasis

In order to more specifically assess the effects of TRC105 on tumor metastasis, we used a clinically relevant mouse model of breast cancer metastasis. Four weeks after transplantation, the primary tumor was removed and mice received adjuvant treatment with TRC105 or human IgG (Fig. 6A). At the time of resection, average tumor volumes were equal in both groups (data not shown). Complete resection of the primary tumor was confirmed by BLI. Six weeks after resection, BLI showed a high number of metastases in the IgG control group, which was strongly reduced in the TRC105 treated group (Fig. 6B). The percentage of mice bearing metastases in the TRC105 treatment group (28.3%) was strongly decreased when compared with the IgG control group (75%, Fig. 6C). Microvessel density in the metastases did not differ between the treatment groups, although only a low number of metastases could be evaluated (data not shown). Additionally, morphology of the primary tumor and metastases was similar in both treatment groups (supplementary Fig. S5). Bioluminescent signals in the TRC105 treated mice were derived from small lesions not invading the underlying tissue at the location of the primary tumor, whereas metastases in the IgG treatment group were found mainly in draining lymph nodes,

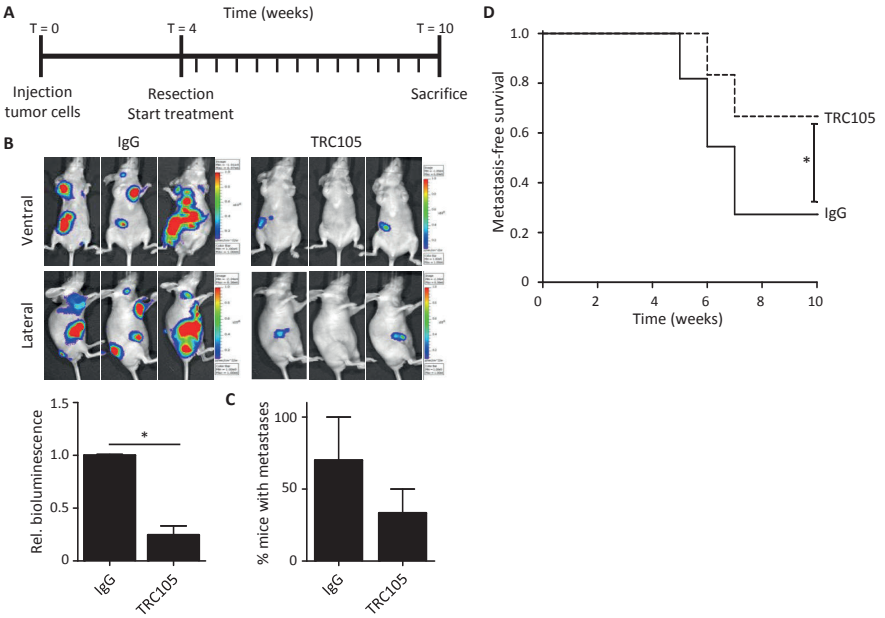

Figure 6 TRC105 treatment inhibits breast cancer metastasis an in adjuvant setting. A. Experimental set-up. Four weeks after tumor transplantation, primary tumors were resected and mice were treated with human IgG or TRC105 for six additional weeks. B. Metastasis formation was followed over time using bioluminescence. Mice treated with TRC105 showed significantly less metastatic lesions when compared with the IgG control group (n= 11-12 mice/group), decreasing the percentage of mice with metastases to 28.3%, compared to 75% in the control mice (C). This results in significantly improved metastasis-free survival of mice treated with TRC105 compared to IgG treatment group (D). Graphs represent mean of 11-12 mice/group from 2 independent experiments. (*, P≤0.05)

bone and peritoneal wall. Only four out of 12 mice treated with TRC105 showed distant metastases, resulting in significantly improved metastasis-free survival of this group (Fig. 6D). These data indicate that adjuvant treatment with TRC105 prevents the development of distant breast cancer metastases.

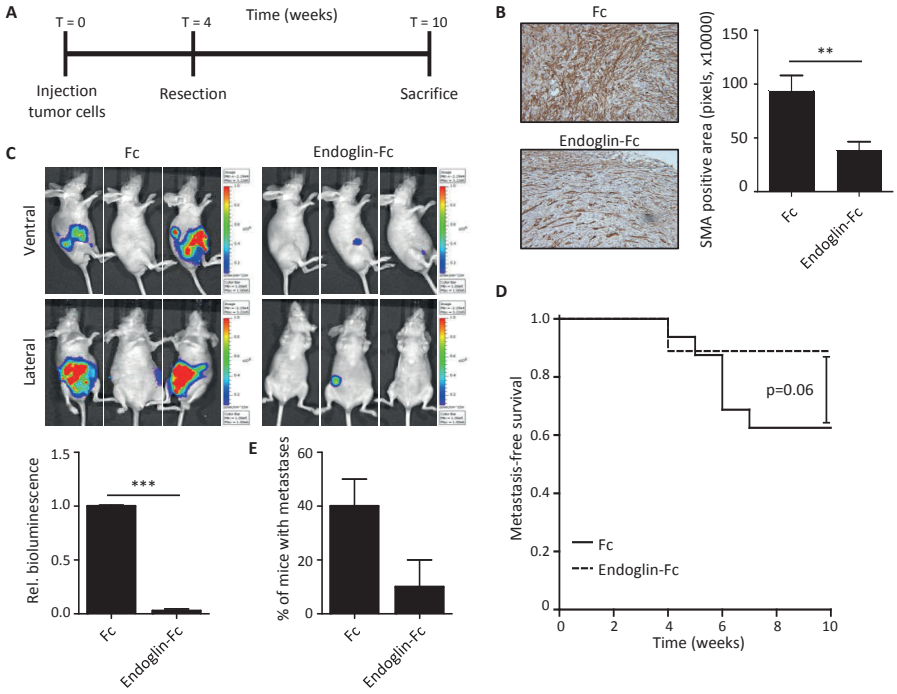

Figure 7 Endoglin-Fc expression decreases metastatic spread of breast cancer cells. A. Experimental set-up. Four weeks after tumor transplantation of cell lines stably expressing Fc or Endoglin-Fc, tumors were resected and metastatic spread was followed for six additional weeks. B. SMA+ stroma content of the primary tumors was strongly decreased by tumoral endoglin-Fc expression, when compared with the Fc group. C. Bioluminescent imaging showed significant reduction of metastatic spread in the endoglin-Fc group when compared with Fc expressing tumors (n= 8 mice/group). D. Expression of endoglin-Fc by the tumor results in improved metastasis-free survival. E. The percentage of mice showing distant metastases was decreased in the endoglin-Fc group by more than 50% compared with Fc. Graphs represent mean of 8 mice/group from 2 independent experiments. (**, P≤0.01, ***, P≤0.001)

Endoglin targeting using endoglin-Fc decreases metastatic spread

To confirm that inhibition of metastasis is indeed caused by targeting endoglin, an alternative approach was used, using an endoglin ligand trap. KEP1-11 cell lines stably expressing either endoglin-Fc or control Fc (supplementary Fig. S6A) were orthotopically transplanted and tumor growth was monitored using bioluminescence and caliper measurements. Comparable to TRC105, endoglin-Fc expression did not affect tumor volume (supplementary Figs. S6B and S6C), while endoglin-Fc strongly decreased primary tumor vascularization (supplementary Fig. S6D). Interestingly, like treatment with TRC105,

mice with endoglin-Fc expressing tumors exhibited a reduced number of metastases (supplementary Fig. S6E).

To assess the effects of endoglin-Fc after primary tumor resection, tumor cells expressing Fc or endoglin-Fc were orthotopically transplanted and allowed to grow for four weeks. Primary tumors were removed and mice were monitored for an additional 6 weeks (Fig. 7A). Upon resection the number of SMA+ CAFs in the primary tumors was significantly lower in the endoglin-Fc group compared with the Fc control group (Fig. 7B). At the end of the experiment bioluminescent signals in the endoglin-Fc group were significantly reduced, compared with the Fc group (Fig. 7C). Expression of endoglin-Fc resulted in decreased metastatic spread and therefore improved metastasis-free survival (Fig. 7D). Additionally, the percentage of mice showing distant metastases decreased by more than 50% in the mice bearing endoglin-Fc expressing tumors (Fig. 7E). Taken together, our results show that targeting endoglin, by TRC105 or endoglin-Fc, strongly decreases the metastatic spread of mouse breast cancer cells *in vivo* and opens possibilities to explore adjuvant TRC105 treatment in breast cancer patients.

Discussion

In this study we show that targeting endoglin, using an antibody or ligand trap, decreases metastatic spread of breast cancer *in vivo*. Combined targeting of the endoglin and VEGF pathway results in decreased angiogenic capacity of human endothelial cells *in vitro*, in a zebrafish model for angiogenesis, and in a mouse model for invasive breast cancer.
In vitro, TRC105 did not inhibit the angiogenic capacity of HUVEC cells. Contrary to our observations, Liu et al. described a significant decrease of HUVEC tube formation, migration and proliferation upon treatment with 100 µg/mL TRC105, a much higher dose than used in this study (31). In the same study additional effects of TRC105 treatment combined with the anti-VEGF agent bevacizumab were reported, supporting our data on redundancy between the endoglin and VEGF signaling pathways (32). The limited effects of TRC105 observed *in vitro* can be explained by the working mechanism of TRC105. Additional to preventing BMP-9 binding to endoglin (20), TRC105 induces antibody dependent cell-mediated cytotoxicity, requiring immune cells. Therefore, the presence of an intact immune system increases TRC105 efficacy (33) and might lead to enhanced effects.
Although xenograft studies showed very promising results for anti-angiogenic therapy and initial responses were observed, patients relapse and actual clinical benefits are limited. In this study we show increased endothelial phosphorylated Smad1 (indicating endoglin signaling) in tumor tissues of cancer patients treated with bevacizumab. In a study on circulating protein biomarkers in TRC105-treated patients the authors reported that certain angiogenic biomarkers, like VEGF, were significantly downregulated shortly after starting TRC105 treatment, indicating inhibition of multiple angiogenic pathways (34). However,

at the end of the study, the same pro-angiogenic factors were upregulated, implying a switch to alternative angiogenic pathways. Therefore, combined targeting of the endoglin and VEGF pathway could result in enhanced and sustained inhibition of angiogenesis. Indeed, in our breast cancer model, tumor angiogenesis was more strongly inhibited by TRC105/SU5416 combination therapy, which unfortunately did not result in decreased tumor volumes. Treatment with bevacizumab, can result in vessel normalization (35, 36). Leaky and irregular tumor vessels partly disappear, but the remaining vessels gain "normal" morphology and pericyte coverage (37). This results in increased blood and nutrient supply to the tumor, sustaining tumor growth, but also enhanced effects of chemotherapy on breast cancer as we could recently show for anti-angiogenic therapy targeting ALK1 (27).
Recently, the first clinical trial assessing TRC105 and bevacizumab combination in patients has been published (21). Of the 38 patients enrolled in this trail, 18 patients showed at least a partial response to treatment. 14 patients had decreased overall tumor burden, of which 10 patients progressed earlier while receiving anti-VEGF treatment, but still responded to TRC105 therapy, suggesting that combination therapy could circumvent therapy resistance. Side effects of combined targeting were limited and not observed more often than with single drug treatment (21), opening doors for clinical use. In addition, a phase-I clinical trial in prostate cancer patients showed almost no classic anti-angiogenesis adverse effects upon TRC105 monotherapy (38). The safety and clinical efficacy of combined TRC105 and anti-VEGF treatment is now being explored in patients with recurrent glioblastoma multiforme (NCT01648348), advanced renal cell cancer (NCT01727089), and other solid tumors (NCT01975519, NCT01306058, NCT01806064).
One of the key findings in this study was the strong inhibition of breast cancer metastasis by endoglin targeting, either by TRC105 or the ligand trap endoglin-Fc. In contrast to our observations, Anderberg et al. reported that endoglin heterozygous mice show increased liver metastasis in Rip-Tag mice (39). Endoglin heterozygote mice develop a hereditary hemorrhagic telangiectasia (HHT) phenotype including vascular malformations (40) and increased vascular permeability (41) possibly resulting in enhanced metastatic spread. When we treated endothelial monolayers with TRC105, trans-endothelial migration of KEP1-11 cells did not change compared with human IgG treatment (data not shown), suggesting that TRC105 does not directly affect endothelial permeability *in vitro*. Another study also showed decreased metastatic spread of prostate cancer in endoglin heterozygous mice (42). These observations imply that both tumor type and method of endoglin targeting could determine metastatic capacity of the cancer cells.
How endoglin mechanistically contributes to metastasis formation is subject of ongoing studies. Since we used a model in which endoglin-Fc is expressed by the tumor cells and therefore present before the angiogenic switch, it is unlikely that decreased metastasis formation is solely due to inhibition of the angiogenic switch. Tumor vessel normalization could prevent tumor cell intravasation and thereby spreading throughout the body. KEP1-11 cells, in contrast to some other breast cancer cells *in vitro* (43), hardly express endoglin or VEGFR2 (supplementary Fig. S7), therefore direct targeting of the tumor cells in our model

is unlikely. However, besides endothelial cells, endoglin is also expressed on other cells in the tumor microenvironment. For example, TRC105 can reduce the number of regulatory T-cells in prostate tumors implying a shift from the presence of regulatory T-cells to cytotoxic T-cells (38). Additionally, macrophages can express endoglin (44), in which it can direct macrophages in either a tumor-suppressive M1 or tumor-promoting M2 phenotype (45).

Our study revealed that treatment with TRC105 or expression of endoglin-Fc resulted in decreased SMA-positive CAF content of the tumors (Figure 5E/7B). The percentage of tumor stroma is known to be a prognostic marker in breast cancer (46, 47). More specifically, CAFs have been shown to play an important role in breast cancer progression and metastasis (reviewed in (48)). We and others (42) have shown that endoglin is expressed by CAFs in diverse types of cancer. A possible explanation for the observed effects could be that treatment with TRC105 or endoglin-Fc might decrease these endoglin expressing CAFs, which stimulate tumor growth and metastasis.

In a phase-I clinical trial, preliminary evidence of clinical activity on pre-existing metastases upon treatment with TRC105 was observed (19). A castrate-resistant prostate cancer patient showed markedly improved metastatic bone lesions upon TRC105 treatment. In another patient, with chemotherapy-resistant uterus carcinoma, a strong decrease in pulmonary metastases was observed after TRC105 treatment. These results, combined with our study showing that even in an adjuvant setting, TRC105 could decrease metastatic dissemination, suggest a role for endoglin in initiating and sustaining distant metastases.

In conclusion, we have shown that dual targeting of the endoglin and VEGF pathway increases anti-angiogenic responses *in vitro* and *in vivo,* compared to monotherapy. Most importantly, we show that targeting of endoglin, either using a neutralizing antibody or a ligand trap, inhibits the metastatic spread of breast cancer *in vivo.* In the light of ongoing trials, our data suggest a potential important role for targeting endoglin in breast cancer metastasis.

Acknowledgements

We thank Jos Jonkers (Netherlands cancer institute, Amsterdam), for providing the KEP1-11 mouse breast cancer cells, Midory Thorikay for generating Fc and endoglin-Fc lentiviral expression constructs, Henry Cheung and Gabri van der Pluijm for practical help in establishing the *in vivo* model and Peter ten Dijke, Hans van Dam and Marie-Jose Goumans (Leiden University Medical Center) for valuable discussions. This work was supported by the Alpe d'huZes/Bas Mulder award 2011 (UL2011-5051) to LH and MP and by a sponsored research grant from Tracon Pharmaceuticals.

Funding

This work was supported by the Alpe d'huZes/Bas Mulder award 2011 (UL2011-5051) to LH and MP and by a sponsored research grant from Tracon Pharmaceuticals.

Conflict of interest

C. Theuer is full time employee of Tracon Pharmaceuticals. All other authors declare no conflicts of interest.

References

1. Torre LA, Bray F, Siegel RL, Ferlay J, Lortet-Tieulent J, Jemal A. Global cancer statistics, 2012. CA Cancer J Clin 2015;65:87-108.
2. Folkman J, Cole P, Zimmerman S. Tumor behavior in isolated perfused organs: in vitro growth and metastases of biopsy material in rabbit thyroid and canine intestinal segment. Ann Surg 1966;164:491-502.
3. Carmeliet P, Jain RK. Angiogenesis in cancer and other diseases. Nature 2000;407:249-57.
4. Folkman J, Merler E, Abernathy C, Williams G. Isolation of a tumor factor responsible for angiogenesis. J Exp Med 1971;133:275-88.
5. Sitohy B, Nagy JA, Dvorak HF. Anti-VEGF/VEGFR therapy for cancer: reassessing the target. Cancer Res 2012;72:1909-14.
6. Sounni NE, Cimino J, Blacher S, Primac I, Truong A, Mazzucchelli G, et al. Blocking lipid synthesis overcomes tumor regrowth and metastasis after antiangiogenic therapy withdrawal. Cell Metab 2014;20:280-94.
7. Bergers G, Hanahan D. Modes of resistance to anti-angiogenic therapy. Nat Rev Cancer 2008;8:592-603.
8. Burrows FJ, Derbyshire EJ, Tazzari PL, Amlot P, Gazdar AF, King SW, et al. Up-regulation of endoglin on vascular endothelial cells in human solid tumors: implications for diagnosis and therapy. Clin Cancer Res 1995;1:1623-34.
9. Miller DW, Graulich W, Karges B, Stahl S, Ernst M, Ramaswamy A, et al. Elevated expression of endoglin, a component of the TGF-beta-receptor complex, correlates with proliferation of tumor endothelial cells. Int J Cancer 1999;81:568-72.
10. Fonsatti E, Jekunen AP, Kairemo KJ, Coral S, Snellman M, Nicotra MR, et al. Endoglin is a suitable target for efficient imaging of solid tumors: in vivo evidence in a canine mammary carcinoma model. Clin Cancer Res 2000;6:2037-43.
11. Li DY, Sorensen LK, Brooke BS, Urness LD, Davis EC, Taylor DG, et al. Defective angiogenesis in mice lacking endoglin. Science 1999;284:1534-7.
12. Arthur HM, Ure J, Smith AJ, Renforth G, Wilson DI, Torsney E, et al. Endoglin, an ancillary TGFbeta receptor, is required for extraembryonic angiogenesis and plays a key role in heart development. Dev Biol 2000;217:42-53.
13. Bourdeau A, Dumont DJ, Letarte M. A murine model of hereditary hemorrhagic telangiectasia. J Clin Invest 1999;104:1343-51.
14. Taranger-Charpin C, Dales JP, Garcia S, Andrac-Meyer L, Ramuz O, Carpentier-Meunier S, et al. The immunohistochemical expression of CD105 is a marker for high metastatic risk and worse prognosis in breast cancers. Bull Acad Natl Med 2003;187:1129-45.
15. Zijlmans HJ, Fleuren GJ, Hazelbag S, Sier CF, Dreef EJ, Kenter GG, et al. Expression of endoglin (CD105) in cervical cancer. Br J Cancer 2009;100:1617-26.
16. Seon BK, Haba A, Matsuno F, Takahashi N, Tsujie M, She X, et al. Endoglin-targeted cancer therapy. Curr Drug Deliv 2011;8:135-43.
17. Paauwe M, ten Dijke P, Hawinkels LJ. Endoglin for tumor imaging and targeted cancer therapy. Expert Opin Ther Targets 2013;17:421-35.
18. Perez-Gomez E, Del CG, Juan FS, Lopez-Novoa JM, Bernabeu C, Quintanilla M. The role of the TGF-beta coreceptor endoglin in cancer. ScientificWorldJournal 2010;10:2367-84.
19. Rosen LS, Hurwitz HI, Wong MK, Goldman J, Mendelson DS, Figg WD, et al. A Phase I First-in-Human Study of TRC105 (Anti-Endoglin Antibody) in Patients with Advanced Cancer. Clin Cancer Res 2012;18:4820-9.
20. Nolan-Stevaux O, Zhong W, Culp S, Shaffer K, Hoover J, Wickramasinghe D, et al. Endoglin Requirement for BMP9 Signaling in Endothelial Cells Reveals New Mechanism of Action for Selective Anti-Endoglin Antibodies. PLoS One 2012;7:e50920.
21. Gordon MS, Robert F, Matei D, Mendelson DS, Goldman JW, Chiorean EG, et al. An Open-Label Phase Ib Dose-Escalation Study of TRC105 (Anti-Endoglin Antibody) with Bevacizumab in Patients with Advanced Cancer. Clin Cancer Res 2014;20:5918-26.
22. Hawinkels LJ, Verspaget HW, van Duijn W, van der Zon JM, Zuidwijk K, Kubben FJ, et al. Tissue level, activation and cellular localisation of TGF-beta1 and association with survival in gastric cancer patients. Br J Cancer 2007;97:398-404.

23. Van Baardewijk LJ, Van der Ende J, Lissenberg-Thunnissen S, Romijn LM, Hawinkels LJ, Sier CF, et al. Circulating bone morphogenetic protein levels and delayed fracture healing. Int Orthop 2013;37:523-7.
24. Hawinkels LJ, Paauwe M, Verspaget HW, Wiercinska E, van der Zon JM, van der Ploeg K, et al. Interaction with colon cancer cells hyperactivates TGF-beta signaling in cancer-associated fibroblasts. Oncogene 2014;33:97-107.
25. Hawinkels LJ, Kuiper P, Wiercinska E, Verspaget HW, Liu Z, Pardali E, et al. Matrix metalloproteinase-14 (MT1-MMP)-mediated endoglin shedding inhibits tumor angiogenesis. Cancer Res 2010;70:4141-50.
26. Derksen PW, Liu X, Saridin F, van der Gulden H, Zevenhoven J, Evers B, et al. Somatic inactivation of E-cadherin and p53 in mice leads to metastatic lobular mammary carcinoma through induction of anoikis resistance and angiogenesis. Cancer Cell 2006;10:437-49.
27. Hawinkels LJ, Garcia d, V, Paauwe M, Kruithof-de JM, Wiercinska E, Pardali E, et al. Activin Receptor-like Kinase 1 Ligand Trap Reduces Microvascular Density and Improves Chemotherapy efficiency to Various Solid Tumors. Clin Cancer Res 2015.
28. Persson U, Izumi H, Souchelnytskyi S, Itoh S, Grimsby S, Engstrom U, et al. The L45 loop in type I receptors for TGF-beta family members is a critical determinant in specifying Smad isoform activation. FEBS Lett 1998;434:83-7.
29. Hawinkels LJ, Zuidwijk K, Verspaget HW, de Jonge-Muller ES, van Duijn W, Ferreira V, et al. VEGF release by MMP-9 mediated heparan sulphate cleavage induces colorectal cancer angiogenesis. Eur J Cancer 2008;44:1904-13.
30. Buijs JT, Matula KM, Cheung H, Kruithof-de Julio M, van der Mark MH, Snoeks TJ, et al. Spontaneous bone metastases in a preclinical orthotopic model of invasive lobular carcinoma; the effect of pharmacological targeting TGFbeta receptor I kinase. J Pathol 2015;235:745-59.
31. Liu Y, Tian H, Blobe GC, Theuer CP, Hurwitz HI, Nixon AB. Effects of the combination of TRC105 and bevacizumab on endothelial cell biology. Invest New Drugs 2014;32:851-9.
32. Pan CC, Kumar S, Shah N, Hoyt DG, Hawinkels LJ, Mythreye K, et al. Src-mediated post-translational regulation of endoglin stability and function is critical for angiogenesis. J Biol Chem 2014;289:25486-96.
33. Tsujie M, Tsujie T, Toi H, Uneda S, Shiozaki K, Tsai H, et al. Anti-tumor activity of an anti-endoglin monoclonal antibody is enhanced in immunocompetent mice. Int J Cancer 2008;122:2266-73.
34. Liu Y, Starr MD, Brady JC, Dellinger A, Pang H, Adams B, et al. Modulation of circulating protein biomarkers following TRC105 (anti-endoglin antibody) treatment in patients with advanced cancer. Cancer Med 2014;3:580-91.
35. Jain RK. Antiangiogenesis strategies revisited: from starving tumors to alleviating hypoxia. Cancer Cell 2014;26:605-22.
36. Arjaans M, Oude Munnink TH, Oosting SF, Terwisscha van Scheltinga AG, Gietema JA, Garbacik ET, et al. Bevacizumab-induced normalization of blood vessels in tumors hampers antibody uptake. Cancer Res 2013;73:3347-55.
37. Goel S, Duda DG, Xu L, Munn LL, Boucher Y, Fukumura D, et al. Normalization of the vasculature for treatment of cancer and other diseases. Physiol Rev 2011;91:1071-121.
38. Karzai FH, Apolo AB, Cao L, Madan RA, Adelberg DE, Parnes H, et al. A phase I study of TRC105 anti-CD105 (endoglin) antibody in metastatic castration-resistant prostate cancer. BJU Int 2014.
39. Anderberg C, Cunha SI, Zhai Z, Cortez E, Pardali E, Johnson JR, et al. Deficiency for endoglin in tumor vasculature weakens the endothelial barrier to metastatic dissemination. J Exp Med 2013;210:563-79.
40. McAllister KA, Grogg KM, Johnson DW, Gallione CJ, Baldwin MA, Jackson CE, et al. Endoglin, a TGF-beta binding protein of endothelial cells, is the gene for hereditary haemorrhagic telangiectasia type 1. Nat Genet 1994;8:345-51.
41. Jerkic M, Letarte M. Increased endothelial cell permeability in endoglin-deficient cells. FASEB J 2015.
42. Romero D, O'Neill C, Terzic A, Contois L, Young K, Conley BA, et al. Endoglin regulates cancer-stromal cell interactions in prostate tumors. Cancer Res 2011;71:3482-93.
43. Henry LA, Johnson DA, Sarrio D, Lee S, Quinlan PR, Crook T, et al. Endoglin expression in breast tumor cells suppresses invasion and metastasis and correlates with improved clinical outcome. Oncogene 2011;30:1046-58.

44. Lastres P, Bellon T, Cabanas C, Sanchez-Madrid F, Acevedo A, Gougos A, et al. Regulated expression on human macrophages of endoglin, an Arg-Gly-Asp-containing surface antigen. Eur J Immunol 1992;22:393-7.

45. Aristorena M, Blanco FJ, de LC-E, Ojeda-Fernandez L, Gallardo-Vara E, Corbi A, et al. Expression of endoglin isoforms in the myeloid lineage and their role during aging and macrophage polarization. J Cell Sci 2014;127:2723-35.

46. de Kruijf EM, Dekker TJ, Hawinkels LJ, Putter H, Smit VT, Kroep JR, et al. The prognostic role of TGF-beta signaling pathway in breast cancer patients. Ann Oncol 2012.

47. Dekker TJ, van de Velde CJ, van Pelt GW, Kroep JR, Julien JP, Smit VT, et al. Prognostic significance of the tumor-stroma ratio: validation study in node-negative premenopausal breast cancer patients from the EORTC perioperative chemotherapy (POP) trial (10854). Breast Cancer Res Treat 2013;139:371-9.

48. Khamis ZI, Sahab ZJ, Sang QX. Active roles of tumor stroma in breast cancer metastasis. Int J Breast Cancer 2012;2012:574025.

Supplementary data

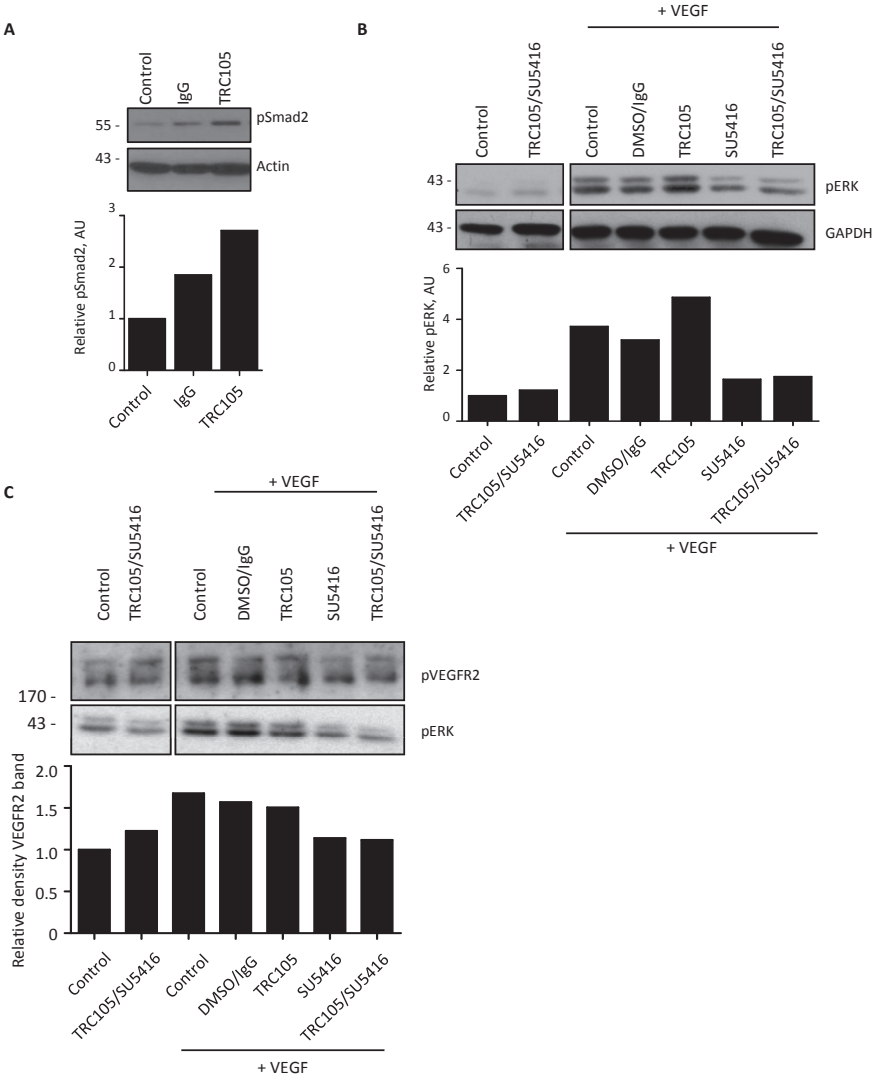

Supplementary figure S1 Densitometric quantification of pSmad2, pERK and pVEGFR2 Tyr1175. A. Overnight treatment with TRC105 increased basal Smad2 phosphorylation in HUVECs. B. Pre-treatment with TRC105 increased VEGF-induced ERK phosphorylation after 10 minutes of stimulation in HUVEC. C. Pre-treatment with TRC105 did not result in increased VEGFR2 phosphorylation on tyrosine1175. Quantifications were corrected for loading control.

Supplementary table S1 QPCR primer sequences

Gene	Forward primer	Reverse primer
Endoglin	tgaatggcaaccacgagc	gcaggatgagaatggcgtc
VEGFR2	tgcgaagccaccgtcaa	ctcgggcgggcgtatttg
GAPDH	atcactgccacccagaagac	atgaggtccaccaccctgtt

QPCR primers as used for detecting mouse endoglin, mouse VEGFR2 and mouse GAPDH.

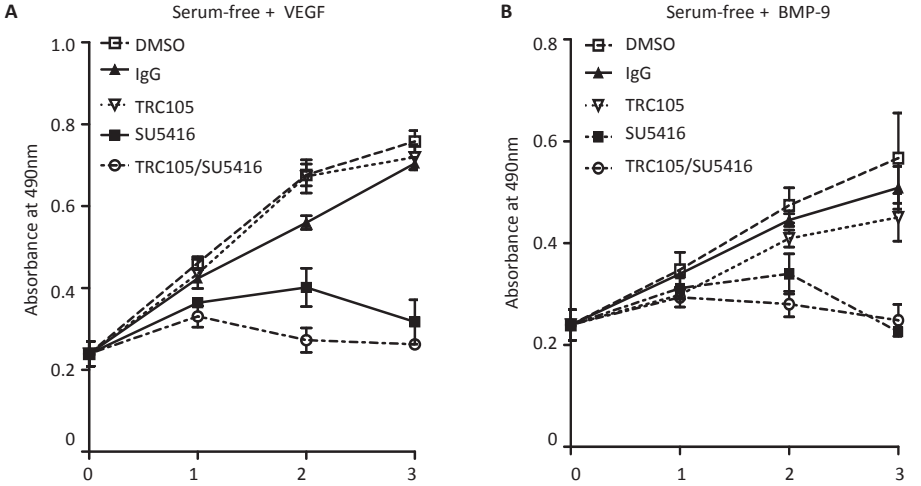

Supplementary figure S2 HUVEC proliferation is dependent on VEGF, but not on the presence of BMP-9. In order to determine the effects of VEGF and BMP-9 on HUVEC proliferation, MTS proliferation assays were performed using serum-free medium (containing BPE). A. When serum-free medium was supplemented with VEGF, HUVEC proliferation was enhanced when compared to serum-free conditions, showing VEGF-dependency. Additionally, as in full serum conditions, targeting VEGF signaling with SU5416 or the combination treatment inhibited proliferation. B. BMP-9 did not affect HUVEC proliferation, although SU5416 and combination treatment still inhibit proliferation in this condition. Graphs are representatives of two independent experiments performed in triplicate.

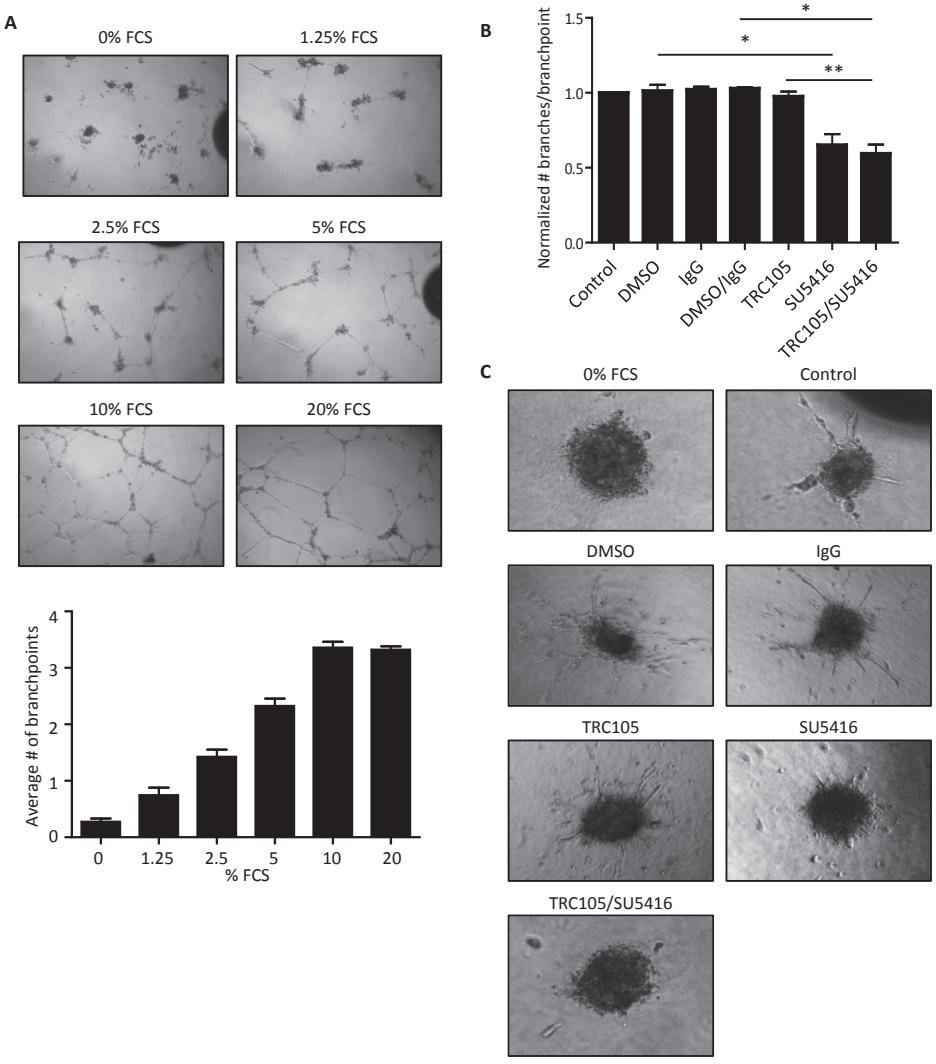

Supplementary figure S3 HUVEC *in vitro* angiogenesis assays. A. To determine the minimal percentage of FCS in the medium required to observe cord formation, a concentration range of FCS was tested. Based on these experiments, 5% FCS was the lowest concentration at which HUVEC cord formation occurred. B. Endothelial cord forming capacity of HUVECs was assessed after overnight incubation with the inhibitors. TRC105 did not affect cord formation, whereas SU5416 treatment decreased the number branches per branchpoint. Data are normalized to control and represent mean of at least 2 independent experiments, performed in triplicate. C. In 3-dimensional HUVEC sprouting assays, sprouting of HUVECs was not affected by TRC105, while SU5416 and especially the TRC105/SU5416 combination significantly reduced sprouting. Data represent mean of three independent experiments, performed in triplicate. (* P≤0,05; ** P ≤0,001)

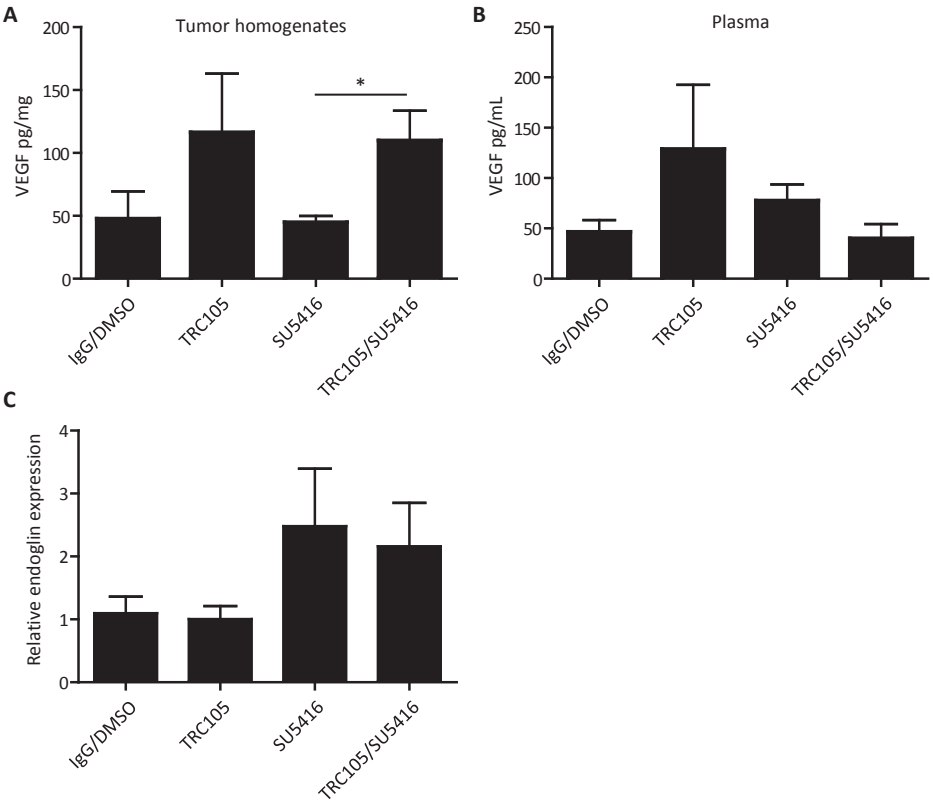

Supplementary figure S4 VEGF and endoglin levels in mouse samples. A. ELISA analysis was performed on tumour homogenates prepared in RIPA lysis buffer. Treatment with TRC105, alone or in combination with SU5416, resulted in increased tumour VEGF levels. B. ELISA analysis on mouse plasma samples. Plasma VEGF levels were increased upon TRC105 treatment, which was reverted after TRC105/SU5416 combination treatment. C. Endoglin mRNA levels were determined using quantitative PCR. Increased endoglin mRNA expression in the groups treated with SU5416, either as monotherapy or in combination with TRC105. (n=4-6 mice/group; *, P≤0.05)

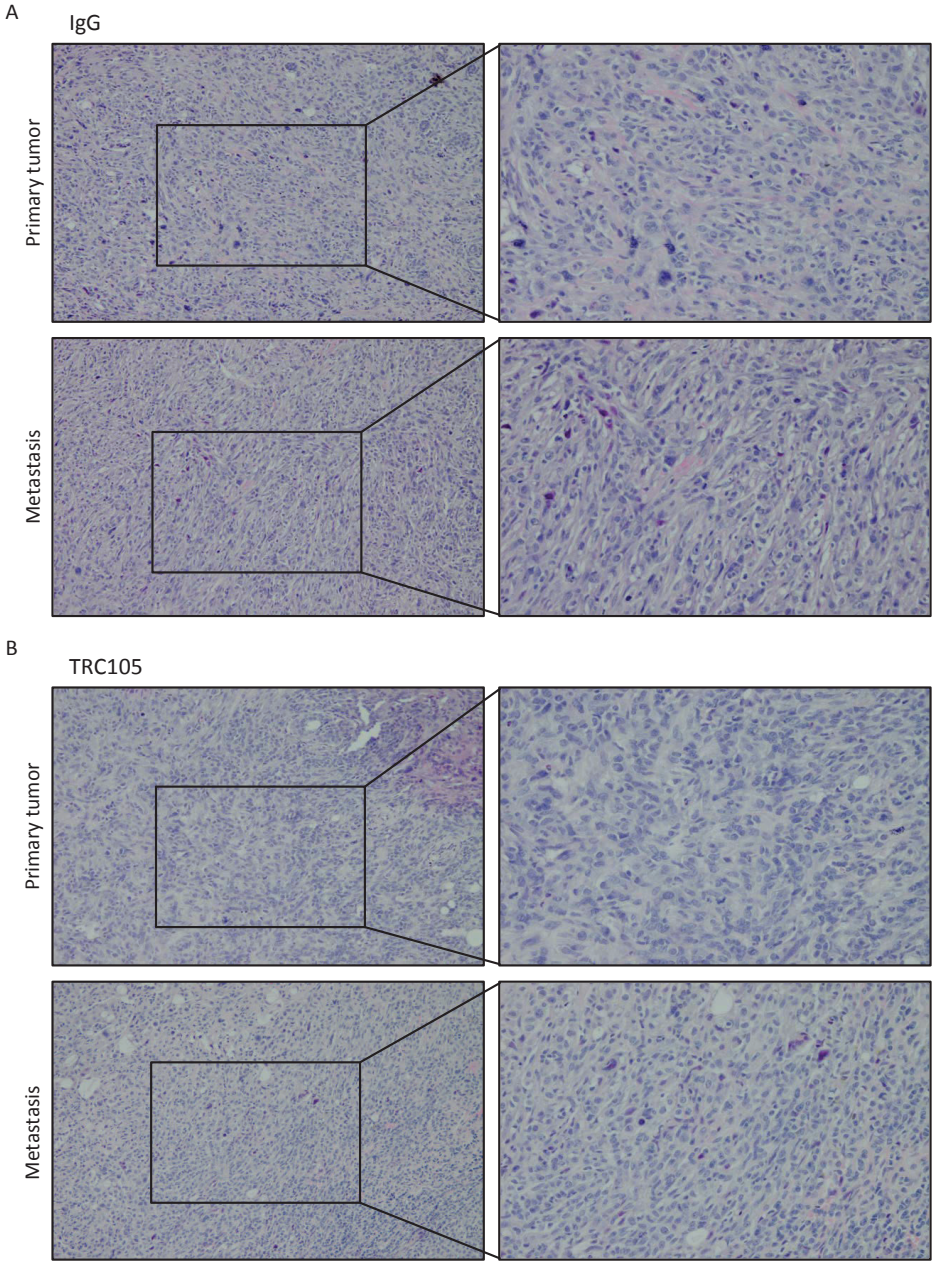

Supplementary figure S5 Histology of primary tumor and metastases. Primary tumors were resected four weeks after transplantation of KEP1-11 cells and metastases were obtained at the end of the experiment. Morphology of primary tumors and metastases were assessed for both the IgG control group (A) and TRC105 treated mice (B).

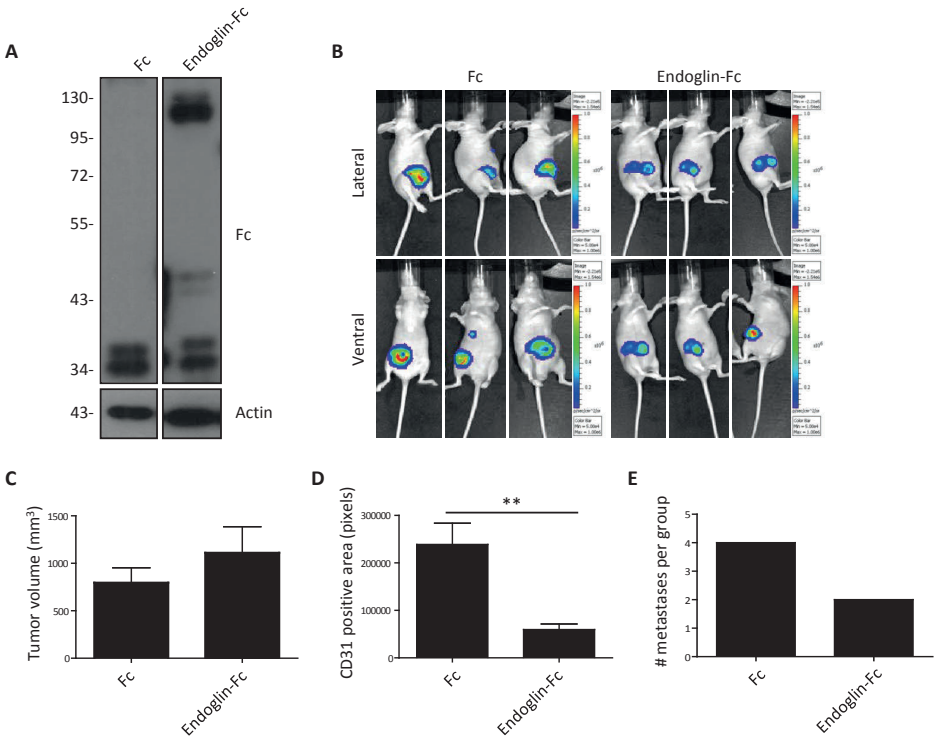

Supplementary figure S6 Endoglin-Fc expression inhibits breast cancer metastasis. KEP1-11 cells were transduced with Fc and endoglin-Fc lentiviral vectors and stable cell lines were created. Expression of the constructs was confirmed using anti-Fc western blot (A). Tumor growth was monitored using bioluminescence (B) and caliper measurement (C). No difference in primary tumor growth was observed, while CD31 immunohistochemical staining revealed a significant decrease in tumor vascular density upon endoglin-Fc expression (D). Mice with endoglin-Fc expressing tumors show reduced number of metastases per group when compared with Fc. (E, n=8 mice/group; **, P≤0.001)

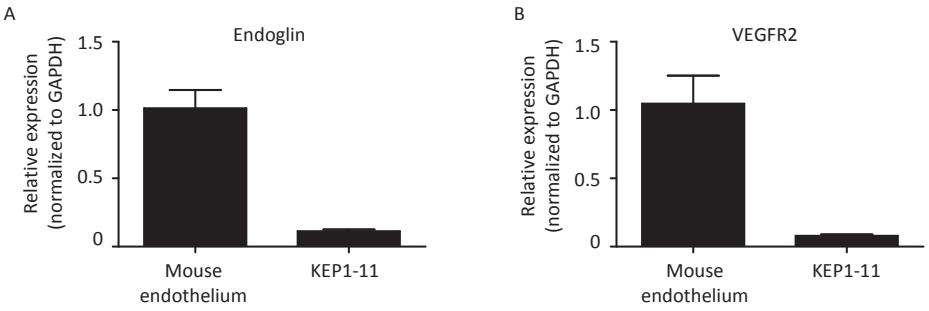

Supplementary figure S7 Endoglin and VEGFR2 mRNA expression in KEP1-11 cells. mRNA expression of endoglin (A) and VEGFR2 (B) by KEP1-11 cells was assessed using quantitative PCR and compared to mouse endothelial cells. Data were normalized to GAPDH expression.